Corrosion Resistance Enhancement for Low Carbon Steel by Gas Phase Coating

Sameer K. Fayyadh[*]
Department of Engineering Machine and Agriculture Equipment,
College of Agricultural Engineering Sciences, University of Baghdad, IRAQ
[*]*samir.faiad@coagri.uobaghdad.edu.iq*

Faras Q. Mohammed
Department of Production Engineering and Metallurgy,
University of Technology, Baghdad, IRAQ

ABSTRACT

Corrosion Resistance Enhancement for low carbon steel is very important to extend its life service, the coating process is one of the methods which can using to achieve this, and it's the most important in surface treatments to improve the properties of metals and alloys surfaces such as corrosion resistance. In this work, low carbon steel was nitrided and coated with nano zinc using gas phase coating technical, to enhance the resistance of corrosion. The process included adding two layers. The first, a nitride layer, was added by precipitating nitrogen (N) gas, and the second, a zinc (Zn) layer, was added by precipitating Zn. The process of precipitating was carried out at different periods (5, 10, and 15 minutes). Scan electron microstructure (SEM), X-ray diffraction (XRD) and corrosion tests were carried out. The SEM and XRD results showed a new microstructure with the emergence of new phases (C_3N_4, $Zn(N_3)_2$, and γN). Also, the results of the corrosion test showed a significant improvement in corrosion resistance through a reduction in the corrosion rate (CR) and corrosion current density (icorr) which reached ($1.598x10^{-3}$ mmpy) and ($1.422x10^{-7}$ Amp/cm^2) respectively, for coated samples, compared with 1.803×10^{-1} and $1.604x10^{-5}$, respectively, for the base metal. also found an appreciable increase in corrosion protection efficiency (CPE), which reached 99.11%.

Keywords: *Carbon Steel; Coating; Corrosion; Gas Phase, Surface Treatment*

ISSN 1823-5514, eISSN 2550-164X

https://doi.org/10.24191/jmeche.v20i2.22059

Received for review: 2022-10-03
Accepted for publication: 2022-12-22
Published: 2023-04-15

Introduction

Low carbon steel (0.25% C max.) is usually applied in numerous industries, including automotive, bridges, ships, storage tanks, large pipes, etc., for its low price and excellent mechanical properties, machinability, weldability, and formability [1]-[2]. However, carbon steel has low resistance to corrosion, which is considered a major economic problem worldwide. Because low carbon steel equipment and machine parts are highly corrosive in chloride or seawater environments, which have varying corrosive levels depending on ion concentration, evaluating corrosion problems in carbon steel is critical [3]-[5]. However, corrosion can be controlled in several ways, including the use of a protective coating, which is the recommended solution for developing materials for resistance to corrosion [6]-[7]. It plays a significant part in forming a barrier between metal surfaces and corrosive media, in addition to improving wear and hardness by modifying the surface's characteristics and forming a new transition region between the deposited layer and the base metal. Metal protection can be achieved by forming thin layers on their surface with thicknesses ranging from a few microns to many atomic layers [8]-[10].

The coating offers protection for the metal by acting either as a sacrificial coating or as a physical barrier. It is essential to have strong adhesion between the protected metals and the coating [11]-[12]. The effectiveness and durability of anti-corrosion coatings depend on the properties of both the substrate and the coating material [10], [13]-[16]. Numerous studies have been done in this field; Ibrahim et al. [17] found that the corrosion resistance of stainless steel 316L was improved after coating it with epoxy-zinc oxide nanocomposite. Also, Dorofeeva et al. [8] reported that stainless steel coated with multi-layers exhibits significantly (tenfold) greater corrosion resistance than the substrate. The coating is made using either the chemical vapour deposition (CVD) or physical vapour deposition (PVD) processes, and sometimes both together, to increase their lifespan. These methods can produce different types of nanostructure coatings. In PVD, the coating material is first evaporated and subsequently condensed onto the substrate. The CVD process, on the other hand, is a chemical reaction that involves the deposition of solid material from a gas or vapour phase onto a heated metal surface [18]-[21]. The deposition of nanostructure coatings on the substrate is usually performed by gas phase deposition procedures. Gas phase deposition has numerous advantages, including high density, chemical stability, good substrate adhesion even on complex shapes, deposition on any desired substrate, and high purity [22]-[24]. Choosing the appropriate coating type for a specific material plays a fundamental role in directly improving or consolidating the surface performance during service. In general, a protective coating made of Zn and Zn alloys is used for a wide variety of applications, including carbon steel to prevent corrosion. Zn

coatings have excellent resistance to corrosion and the possibility for economic competitiveness [25]-[29]. On the other hand, adding nitrogen gas to steel through the nitriding process leads to improving the surface properties, such as increasing the corrosion resistance by the formation of nitriding layers [30]-[31]. This work is aimed at protecting low carbon steel from corrosive ingredients present in the working environment and enhancing the corrosion resistance through the deposition of the layers of coating of N and Zn using the gas-phase method.

Materials and Methods

Materials

The low-carbon steel AISI 1020 was used as a substrate material in all of the practical experiments. The chemical analysis of low carbon steel is shown in Table 1 and compared with American Standard [32]. N, Ammonia (NH_3) gas, and Zn solid target with a purity of 99.9% were supplied from a local market.

Table 1: Chemical composition of AISI 1020

Elements	C	Mn	P	S	Fe
Actual value %	0.20	0.55	0.01	0.04	Bal.
Standard value %	0.18-0.23	0.3-0.6	0.04 max.	0.05 max	Bal.

Methods

Samples prepared

Specimens that were used for microstructure tests were cut with dimensions of 10x10x3 mm, while specimens used for the corrosion test were cut with dimensions of 15x15x3 mm. All specimens were conventionally prepared before being ready for the nitriding and Zn coating processes.

Coating processes

The nitriding process was performed by the CVD technique. For this process, a GSL-1600-60X high-temperature vacuum tube furnace was utilized. It consists of a tube with a length of 1000 mm, a 60 mm diameter, and an inner diameter of 54 mm. Using a high-precision SCR (Silicon controlled Rectifier-digital controller) power controller (±1 ºC) accuracy, the temperature of the GSL 1600-60X tube furnace is controlled. A two-stage rotary vacuum pump with a 120 SLPM (Standard Litter Per Minute) capacity was equipped for the furnace. In the nitriding process, NH_3 (gas) was utilized to supply the gas reactant with atoms of nitrogen, while N_2 gas was employed as a carrier gas to carry out the process. To reduce residual stresses, all nitriding samples were heated to 550 ºC. To deposit a thin film of the Zn

nano-structure coating, the VTC-16-D device was used, which, a desktop Plasma Sputtering Coater involving a height-adjustable sample holder and a 3-target head, especially suitable for coating conductive metal film samples. The parameters of the sputtering process were vacuum pressure of 10-1 Torr, current of 18 mA, and 2 cm^3/min of the flow rate of argon gas. The coating processes were performed with different deposition times of 5, 10, and 15 minutes.

Characterizations

Microstructure and X-ray diffraction

XRD analysis was carried out using an x-ray diffractometer, type XRD-6000 Shimadzu, with Cu-Kα radiation and a 0.154 nm angle of incident. Also, a microstructure examination was carried out using a Tescan VEGA 3SB SEM with an accelerating voltage range of 200 v to 30 kv and a power magnification range of 6x to 100000x.

Electrochemical performance

The Tafel polarization test was used to evaluate the coating's ability to protect and prevent low-carbon steel from corrosion. The experiment was conducted using CHI 604E POTENTIOSTAT. The conventional three-electrode electrochemical cell was used to measure the test output. The electrochemical cell includes, (Pt) as a counter electrode, saturated Ag/AgCl as a reference electrode, and a sample holder as the working electrode. The cell parameters were the scanning of electrode potential between -1.6 and +0.6 V at a scan rate of 0.01 $V.s^{-1}$ and 1.0 cm^2 was the area of exposed work to the aqueous solution. All specimens were examined at room temperature and using an aqueous solution of 3.5% NaCl. It's a simulated marine environment which is the most corrosive medium for the steel substrate.

Results and Discussion

XRD analysis

The XRD analysis and identifying the presence phases were done using the International Center for Diffraction Data (ICDD) cards and Match! 3 software. Figure 1 shows the XRD pattern that was conducted for the nitriding and Zn-coated low carbon steel samples. Both samples confirm the existence of α-Fe as the original alloy substance at 2θ angles of 64.41 and 44.63 with an index of (200) and (101), respectively (from ICDD card no. 00-006-0696). Regardless of the Fe phase, the two analyzed samples can show considerable differences in the microstructure and phases existing in the figure. The nitride sample's XRD analysis revealed the presence of the C_3N_4 phase at 2 angles of, 62.47, 37.026, and 30.06 with (112), (110), and (100) indices, respectively (from ICDD card no. 00-053-0671). This proves that the

intermixing was done between the nitriding layer and substrate through the process of nitriding under the process condition. Additionally, the γN phase was observed in this pattern at 2θ angles of 54.02, 43.051, and 35.485, with (200), (111), and (101) indices. The XRD patterns for the Zn-N coatings deposited under different conditions are also shown in Figure 1. These phases were formed as a result of the interactions between the substrate and the coating materials under the conditions of the deposition processes. The nitriding and coating of low carbon steel by zinc confirmed the presence of several compounds in addition to the C_3N_4 and γN phases that were formed as a result of the nitriding processes. The XRD analysis of the other sample revealed the presence of a new phase in this pattern in comparing to other nitriding samples, with three distinct peaks for $Zn(N_3)_2$ identified at 47.319, 33.44, and 22.44 with indices of (123), (210), and (200) that may be identified [from ICDD card no. 00-023-0740]. The XRD analysis can be used to find many information regarding material crystallography and the microstructure examination. In this regard, the diffraction peak intensities corresponding to some of the presented phases was found to be gradually decrease and a peak-broadening were reduced for these samples as it was shown in Figure 1. Also, the shifting in the diffraction peaks angles for these samples (at 10 minutes toward higher diffraction angles was observed as the deposition time was increased to 20 minutes. indicating a decrease in the coating lattice parameter which indicates that a polycrystalline structure was developed for this sample in Figure 1.

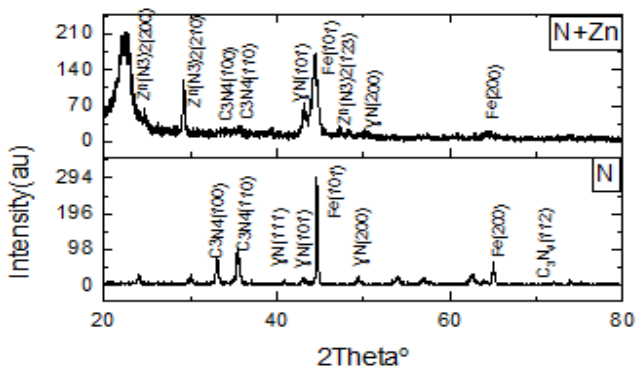

Figure 1: XRD analysis for surface treated samples

SEM

Figures 2, 3, and 4 show the morphology of the low carbon steel surface, which was nitrided and coated with a film of Zn at different deposition times. In Figure 2, the surface morphology after nitriding treatments at 500 °C shows a dense structure for the layer of nitrogen expanded austenite (γN),

accompanied by a uniform nitriding layer with a very smooth finish of the surface, and no visible cracks were observed. It was due to the intensive nitride precipitation that occurred that expanded austenite was also detected, as was evidenced in XRD test results. The surface morphology for the Zn coating on the nitriding low carbon steel surface is shown in Figures 3 and 4 with different deposition times. Deposition of Zn at a low deposition time will result in a surface that is characterized by an amorphous matrix that contains a fine nanocrystal fiber structure that is visible in SEM images of this sample. Also, a longitudinal micro void can be detected in this image that formed in the coating's surface because of the short deposition period, which caused a decrease in the amount of deposited coating. A so-called thin film of the coating was produced with an 8.3 µm thickness for the zinc coating layer, which was determined by the longitudinal gap shown in Figure 2. As the deposition time for Zn coatings increased to 20 minutes, a higher deposition rate occurred, which resulted in a change in the morphology towards a denser microstructure, more uniform coating, a much coarser surface finish than the former surface layer, and no visible microvoids. Also, a nano-crystalline fiber structure can be detected. A higher deposition time offers more deposition, which can increase the average coating thickness. It was revealed that the Zn coating's thickness was obtained from coating for 20 minutes (Figure 5). and was approximately 23 µm. This thickness, regarded as relatively large, was obtained as a result of higher deposition time for the zinc coating layer.

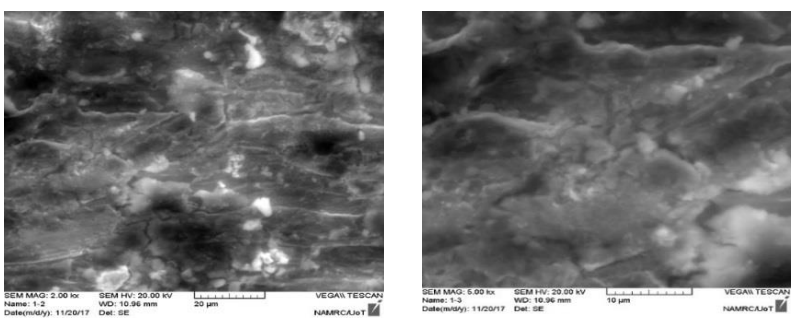

Figure 2: SEM micrograph for nitriding low carbon steel surface with different magnifications

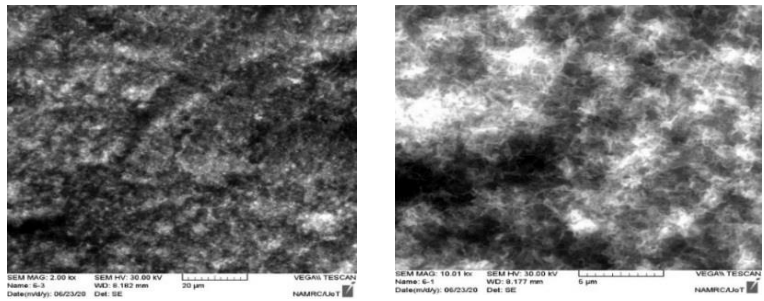

Figure 3: SEM micrograph for nitriding and Zn coated low carbon steel surface at 10 minutes with different magnifications

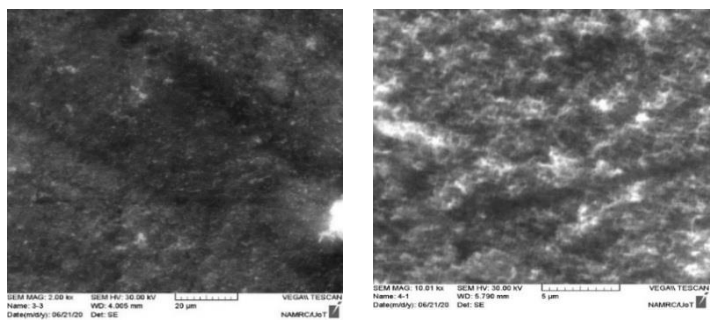

Figure 4: SEM micrograph for nitriding and Zn coated low carbon steel surface at 20 minutes with different magnifications

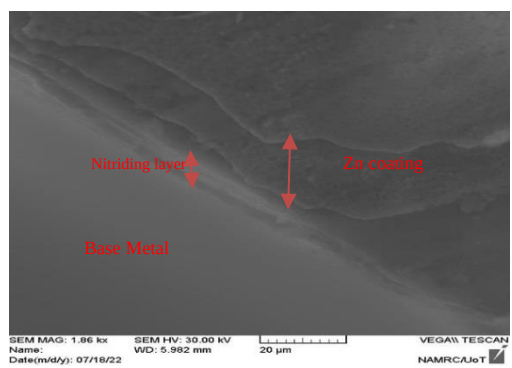

Figure 5: Cross section SEM image for nitriding and Zn coated low carbon steel surface at 20 minutes

Corrosion behaviour

Figure 6 shows the Tafel polarization curves for coated and uncoated low carbon steel. It provides several significant parameters, such as corrosion current density (icorr), corrosion potential (Ecorr), and corrosion rate (CR), which was calculated by using the following equation [33].

$$CR = \frac{K1(icorr)\ EW}{\rho} \quad (1)$$

where CR: corrosion rate (mm/y), K1= $3.27x10^{-3}$ mm g/μA cm y, EW: Equivalent weight (the atomic weight of the element in gram/ valence of the element), ρ: density in g/cm^3, and to evaluate the protective effect of coatings on low carbon steel, the criterion of corrosion protection efficiency (CPE) was also used and determined using the following equation [16], [34].

$$CPE(\%) = \frac{\left(I^o\text{corr} - I^C\ corr\right)}{I^o corr} 100\% \quad (2)$$

where I^{o}corr represents the corrosion current density (Amp/cm^2) for the uncoated sample, while I^{c}corr represents the corrosion current density (Amp/cm^2) of the coated specimens. According to Figure 6, the (icorr) for coated samples shifts to a lower value compared with (icorr) for uncoated ones, which means that the corrosion resistance was increased after the coating processes, and it was observed that this increased depending on the parameters of the coating processes. From Table 2, it can be seen that the (icorr) ($1.604x10^{-5}$ Amp/cm^2) of the uncoated sample was significantly higher compared with the (icorr) ($3.657x10^{-6}$) for the sample that was only nitrided and ($1.422x10^{-7}$ Amp/cm^2) for samples that were coated with Zn after the nitriding process, which demonstrated the protective effect of the coating processes. In another word, the (CR) significantly decreased from ($1.80x10^{-1}$ mmpy) for uncoated samples to ($4.111x10^{-2}$ mmpy) for the sample that was only nitrided and ($1.598x10^{-3}$ mmpy) for samples that were coated with Zn after the nitriding process, as shown in Table 2. Also, it was observed that incorporation of N and N + Zn nano-crystalline fiber structure into the substrate surface led to the addition of a significant decrease in (CR) and (icorr), which led to a significant increase in CPE, reaching 77.20% for N coating and 99.11% for N + Zn coating. This result was in agreement with the findings of Zhang et al. [16]. The high CPE and low CR indicate that the coating by N+Zn causes the formation of a barrier that has a superior ability to prevent the penetration of corrosive species and, therefore, provides excellent resistance to corrosion due to the barrier properties offered by this coating. Compared between coated and uncoated samples, the coated one showed lower CR and higher CPE. This demonstrates the effectiveness of utilizing zinc as an insulating coating layer to prevent the transition of

corrosive media to the substrate, thereby enhancing the resistance to corrosion. Additionally, the zinc coating acts as a sacrificial or cathodic protection to prevent iron corrosion because zinc is more electronegative (more reactive) than steel in the galvanic series, which means the zinc coating acts as an anode. Also, it was observed that zinc coating after nitride achieved better results than only the nitride process, where the (icorr) ($1.422x10^{-7}$) and CR ($1.598x10^{-3}$) lower compared to the (icorr) ($3.657x10^{-6}$) and CR ($4.111x10^{-2}$) for only nitride. Also, the zinc coating after nitride achieved a higher corrosion protection efficiency (99.11%) compared to (77.20%) for only the nitriding process. On the other hand, it was observed that both (icorr) and CR were significantly reduced while CPE highly increased as deposition time increased, to clarify this: as it was noted in the previous section, the thickness of the coating increases as time deposition increases; therefore, if a zinc coating is exposed to severe damage, the steel won't corrode until the surrounding zinc has been consumed. So, the amount of protection provided by a zinc coating is roughly proportional to the coating's thickness. finally, the results showed that the coating using N+Zn nano-crystalline fiber structure could be an active barrier and anti-corrosion performance enhancer that enhances the corrosion resistance of the low carbon steel, these results are in agreement with what was obtained by Dorofeeva et al. [8] and Ibrahim et al. [17].

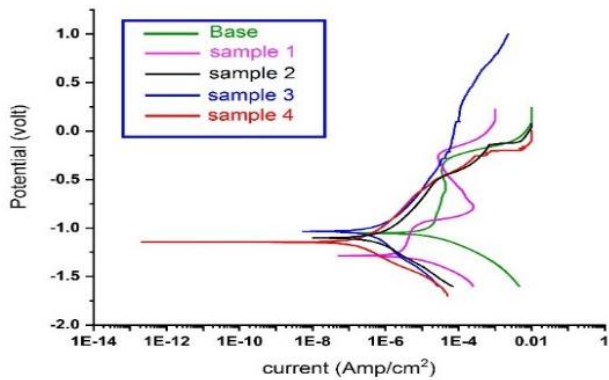

Figure 6: Tafel plots of base metal and coated samples at different deposition times measured in 3.5 % NaCl aqueous solutions at room temperature

Table 2: Tafel plots parameters

Sample no.	Process	Time	Ecorr. (volt)	icorr. (Amp/cm^2)	Corr rate (mmpy)
Base metal	uncoated	/	-1.055	$1.604x10^{-5}$	$1.803x10^{-1}$
1	N	5	-1.288	$3.657x10^{-6}$	$4.111x10^{-2}$
2	N+Zn	5	-1.102	$4.777x10^{-7}$	$5.370x10^{-3}$
3	N+Zn	10	-1.035	$3.809x10^{-7}$	$4.282x10^{-3}$
4	N+Zn	15	-1.144	$1.422x10^{-7}$	$1.598x10^{-3}$

Conclusions

From the previous results, it can be concluded, that the protection of low carbon steel from corrosion can be achieved by nitriding and the Zn coating process, where the coating led to a significant reduction in corrosion rates and a clear increase in the corrosion protection efficiency as follows:

1. Decrease the corrosion rate from $1.803x10^{-1}$ (mmpy) for uncoated samples to $4.111x10^{-2}$ (mmpy) for samples treated with nitridation only.
2. Reduce the corrosion rate from $1.803x10^{-1}$ (mmpy) for uncoated samples to $1.598x10^{-3}$ (mmpy) for zinc-coated samples after nitridation.
3. Compared with uncoated samples, the corrosion protection efficiency for samples treated with only nitride reached 77.20%, while it increased even more in samples that were coated with zinc after the nitridation process, reaching 99%.
4. A greater reduction was achieved in corrosion rate ($5.370x10^{-3}$) and a greater increase in corrosion protection efficiency (86.93%) for samples that were zinc-coated after nitriding, compared to corrosion rate ($4.111x10^{-2}$) (mmpy) and corrosion protective efficiency (77.2%) for samples that were only nitrided at the same period of deposition.
5. Corrosion rates decreased as Zn deposition time increased, with corrosion rates of $5.370x10^{-3}$, $4.282x10^{-3}$, and $1.598x10^{-3}$ for deposition times of 5, 10, and 15 minutes, respectively, and protection efficiency increased for the same periods.

Contributions of Authors

The authors confirm the equal contribution in each part of this work. All authors reviewed and approved the final version of this work.

Funding

This work received no specific grant from any funding agency.

Conflict of Interests

All authors declare that they have no conflicts of interest.

Acknowledgment

The authors would like to thank the microscopy and X-ray laboratories at the Nano Technology and Advanced Materials Research Center, University of Technology, as well as the corrosion laboratory in the Materials Research Department of the Science and Technology Authority.

References

[1] A. E. S. Fouda, S. M. A. Motaal, A. S. Ahmed, and H. B. Sallam, "Corrosion Protection of Carbon Steel in 2M HCl Using Aizoon canariense Extract," *Biointerface Research in Applied Chemistry*, vol. 12, no. 1, pp. 230–243, 2021, doi: 10.33263/briac121.230243.

[2] A. N. Mohsin, H. M. Yousif, and S. S. Ahmed, "Investigation of the Diffusion Depth of Ni-Cu Thermal Spray Coating for the Low Carbon Steel," *Engineering and Technology Journal*, vol. 39, no.11, pp. 1734–1739, 2021.

[3] Esmaeil Jafari, "Improving the Corrosion Resistance of Carbon Steel by Ni–P Nano-Structured Coating," *Russian Journal of Electrochemistry*, vol. 57, no. 6, pp. 663–670, 2021, doi: 10.1134/S1023193520120083.

[4] J. T. Stephen, A. Adebayo, and B. S. Oluwadare, "Corrosion Inhibition of Alkaline Solution on Low Carbon Steel In Local Water (Oku River)," *International Journal of Scientific and Technical Research in Engineering*, vol. 14, no .4, pp. 1-7, 2019.

[5] N. Ali, T. E. Putra, Husaini, V. Z. Iskandar, and S. Thalib, "Corrosion Rate of Low Carbon Steel for Construction Materials in Various NaCl Concentrations," In *IOP Conference Series: Materials Science and Engineering*, vol. 536, no. 1, pp. 012015, 2019, doi: 10.1088/1757-899X/ 536/1/012015.

[6] O. A. Abdulrazzaq, S.M. Saeed, Z.H. Ali, S.A. Tuma, O.A. Ahmed, A.A. Faridoon, and S.K .Abdulridha, "Enhancement of low carbon steel corrosion resistance in acidic and saline media using superhydrophobic

nanocomposite", *Experimental and Theoritical Nanotechnology*, vol. 5, no. 1, pp. 77-78, 2021, doi.org/10.56053/5.1.77.

[7] Y. Tian, Z. Bi, and G. Cui, "Study on the corrosion resistance of graphene oxide-based epoxy zinc-rich coatings," *Polymers*, vol. 13, no. 10, pp. 1–20, 2021, doi: 10.3390/polym13101657.

[8] T. Dorofeeva, T. Gubaidulina, V. Sergeev, and M. Fedorischeva, "Si-Al-N-O Multi-Layer Coatings with Increased Corrosion Resistance Deposited on Stainless Steel by Magnetron Sputtering," *Metals*, vol. 12, no. 2, pp. 254, 2022, doi.org/10.3390/ met12020254

[9] A. A. H. Kadhum and M. Ahmed, "Corrosion Inhibition of Low Carbon Steel in HCl Medium Using Thiadiazole derivative: Weight loss, DFT Studies and Antibacterial Studies," *International Journal of Corrosion and Scale Inhibition*, vol. 10, no. 4, pp. 1812–1828, 2021, doi: 10.17675/2305-6894-2021-10-4-27.

[10] G. Lazorenko, A. Kasprzhitskii, and T. Nazdracheva, "Anti-corrosion coatings for protection of steel railway structures exposed to atmospheric environments: A review," *Construction and Building Materials*, vol. 288, pp. 123115, 2021, doi: 10.1016/j.conbuildmat.2021. 123115.

[11] K. K. Maniam and S. Paul, "Corrosion Performance of Electrodeposited Zinc and Zinc-Alloy Coatings in Marine Environment," *Corrosion and Materials Degradation*, vol. 2, no. 2, pp. 163–189, 2021, doi: 10.3390/ cmd2020010.

[12] S. Fryska and J. Baranowska, "Corrosion properties of S-phase/Cr2N composite coatings deposited on austenitic stainless steel," *Materials*, vol. 15, no. 1, pp. 266, 2022, doi: 10.3390/ma15010266.

[13] A. A. Ugla, M. I. Hasan, Z. A. Ibrahim, D. J. Kamil, and H. J. Khudair, "Effects of nano coating on the mechanical properties of turbine blades: A review," *Journal of Mechanical Engineering Research and Developments*, vol. 44, no. 4, pp. 134–144, 2021.

[14] Y. I. Kuznetsov and G. V Redkina, "Thin Protective Coatings on Metals Formed by Organic Corrosion Inhibitors in Neutral Media," *Coatings*, vol. 12, no.2, pp. 149, 2022, doi.org/10.3390/ coatings12020149.

[15] J. N. Panda, B. C. Wong, E. Medvedovski, and P. Egberts, "Enhancement of tribo-corrosion performance of carbon steel through boronizing and BN-based coatings," *Tribology International*, vol. 153, pp. 106666, 2021, doi: 10.1016/j.triboint.2020.106666.

[16] M. Zhang, H. Wang, T. Nie, J. Bai, F. Zhao, and S. Ma, "Enhancement of barrier and anti-corrosive performance of zinc-rich epoxy coatings using nano-silica/graphene oxide hybrid," *Corrosion Reviews*, vol. 38, no. 6, pp. 497–513, 2020, doi: 10.1515/corrrev-2020-0034.

[17] N. F. Ibrahim, W. R. W. Abdullah, M. S. Rooshde, M. S. M. Ghazali, and W. M. N. W. Nik, "Corrosion inhibition properties of epoxy-zinc oxide nanocomposite coating on stainless steel 316l," In *Solid State Phenomena*, vol. 307, pp. 285–290, 2020, doi: 10.4028/www.scientific.

net/SSP.307.285.

[18] D. Lu, Y. Huang, J. Duan, and B. Hou, "A zinc-rich coating fabricated on a magnesium alloy by oxide reduction," *Coatings*, vol. 9, no. 4, pp. 278, 2019, doi: 10.3390/coatings9040278.

[19] A. D. Thamir, "Corrosion Resistance Enhancement in Acidic solution for Austenitic Stainless Steel by Gas- Phase Hybrid Deposition Process," *Engineering and Technology Journal*, vol. 35, no. 8, pp. 788-794, 2017, doi.org/10.30684/etj.35.8A.1

[20] A. Baptista, F. Silva, J. Porteiro, J. Míguez, and G. Pinto, "Sputtering physical vapour deposition (PVD) coatings: A critical review on process improvement andmarket trend demands," *Coatings*, vol. 8, no. 11, pp. 402, 2018, doi: 10.3390/COATINGS8110402.

[21] A. D. Thamir, A. J. Haider, F. Q. Mohammed, and K. M. Chahrour, "Hybrid gas phase Ti-B-C-N coatings doped with Al," *Journal of Alloys and Compounds*, vol. 723, pp. 368–375, 2017, doi: 10.1016/j.jallcom. 2017.06.281.

[22] G. V. Pachurin, N. A. Kuz'min, A. A. Filippov, and T. V. Nuzhdina, "Mechanical Characteristics of Steels with a Gas-Phase Nickel Coating," *Russian Metallurgy*, vol. 2019, no. 13, pp. 1407–1409, 2019, doi: 10.1134/S0036029519130251.

[23] V. N. Popok and O. Kylián, "Gas-Phase Synthesis of Functional Nanomaterials," *Applied. Nano*, vol. 1, no. 1, pp. 25–58, 2020, doi: 10.3390/applnano1010004.

[24] Y. Huttel, L. Martínez, A. Mayoral, and I. Fernández, "Gas-phase synthesis of nanoparticles: Present status and perspectives," *MRS Communications*, vol. 8, no. 3, pp. 947–954, 2018, doi: 10.1557/mrc. 2018.169.

[25] J. Votava, V. Kumbár, A. Polcar, and M. Fajman, "Change of Mechanical Properties of Zinc Coatings after Heat Treatment," *Acta Technologica Agriculturae*, vol. 23, no. 1, pp. 7–11, 2020, doi: 10.2478/ata-2020-0002.

[26] S. C. Shi, P. W. Huang, and J. H. C. Yang, "Low-temperature large-area zinc oxide coating prepared by atmospheric microplasma-assisted ultrasonic spray pyrolysis," *Coatings*, vol. 11, no. 8, pp. 1001, 2021, doi: 10.3390/coatings11081001.

[27] M. Khiari, M. Gilliot, M. Lejeune, F. Lazar, and A. Hadjadj, "Preparation of Very Thin Zinc Oxide Films by Liquid Deposition Process: Review of Key Processing Parameters," *Coatings*, vol. 12, no. 1, pp. 1–24, 2022, doi: 10.3390/coatings12010065.

[28] C. M. P. Kumar, M. P. G. Chandrashekarappa, R. M. Kulkarni, D. Y. Pimenov, and K. Giasin, "The effect of zn and zn–wo3 composites nano-coatings deposition on hardness and corrosion resistance in steel substrate," *Materials*, vol. 14, no. 9, pp. 2253, 2021, doi: 10.3390/ma1 4092253.

[29] N. Boshkova, K. Kamburova, T. Radeva, and N. Boshkov, "Hybrid zinc-based multilayer systems with improved protective ability against localized corrosion incorporating polymer-modified zno or cuo particles," *Coatings*, vol. 11, no. 10, pp. 1223, 2021, doi: 10.3390/coatings11101223.

[30] V. Timm Bonow, D. Stefani Maciel, A. Zimmer, and C. G. Zimmer, "Nitriding in low carbon steels using non-toxic salt baths," *Revista Liberato*, vol. 1, pp. 177–186, 2019, doi: 10.31514/rliberato. 2019v20n34.p177.

[31] P. Landgraf, *T.* Bergelt, L. Rymer, C. Kipp, T. Grund, G. Bräuer and T. Lampke, "Evolution of Microstructure and Hardness of the Nitrided Zone during Plasma Nitriding of High-Alloy Tool Steel," *Metals*, vol. 12, no. 5, pp. 866, 2022, doi: 10.3390/met12050866.

[32] A. Afnor, "Handbook of Comparative World Steel Standards, 5th Edition," *Handbook of Comparative World Steel Standards, 5th Ed.*, 2016, doi: 10.1520/ds67d-eb.

[33] G. ASTM, "Standard practice for calculation of corrosion rates and related information from electrochemical measurements," *G102-89*, Reapproved 2004, pp. 1–7, 2015, doi: 10.1520/G0102-89R15E01.2.

[34] I. Chung, V. Hemapriya, K. Ponnusamy, N. Arunadevi, Subramanian Chitra, Chi Hee-Youn, Seung-Hyun Kim, and M. Prabakaran, "Assessment of low carbon steel corrosion inhibition by eco-friendly green chaenomeles sinensis extract in acid medium," *Journal Electrochemical Science and Technology*, vol. 9, no. 3, pp. 238–249, 2018, doi: 10.5229/JECST.2018.9.3.238.